Liver Segmentation Approach Using Graph Cuts and Iteratively Estimated Shape and Intensity Constrains

Ahmed Afifi[1] and Toshiya Nakaguchi[2]

[1] Faculty of Computers and Information, Menoufia University, Egypt
[2] Graduate School of Engineering, Chiba University, Japan

Abstract. In this paper, we present a liver segmentation approach. In which, the relation between neighboring slices in CT images is utilized to estimate shape and statistical information of the liver. This information is then integrated with the graph cuts algorithm to segment the liver in each CT slice. This approach does not require prior models construction, and it uses single phase CT images; even so, it is talented to deal with complex shape and intensity variations. Moreover, it eliminates the burdens associated with model construction like data collection, manual segmentation, registration, and landmark correspondence. In contrast, it requires a low user interaction to determine the liver landmarks on a single CT slice only. The proposed approach has been evaluated on 10 CT images with several liver abnormalities, including tumors and cysts, and it achieved high average scores of 81.7 using MICCAI-2007 Grand Challenge scoring system. Compared to contemporary approaches, our approach requires significantly less interaction and processing time.

1 Introduction

In liver CAD systems, the liver segmentation is the first and essential process, and its accuracy is of special significance. However, this process is difficult because of low contrast between the liver and surrounding tissues , great differences in liver shape and intensity , and the existence of liver abnormalities. In literature, there are many attempts to solve the liver segmentation problem and various approaches have been proposed, including intensity or texture based approaches, deformable and statistical model-based approaches, and probabilistic atlases based approaches. Survey and comparison of different liver segmentation approaches have been presented in [1,2].

In the intensity based approaches, one or multiple intensity thresholds, region growing, or watershed methods are applied to extract an initial binary volume which consequently refined using morphological filters or knowledge-based approaches. Recent approaches of this category have been proposed in [3,4], and by Beck and Aurich in [2]. In the deformable model-based approaches, an initial contour or surface is deformed to minimize a predefined energy function. In [5,6], deformable models have been coupled with shape models and intensity thresholding to perform liver segmentation. Additionally, Gradient vector flow (GVF)

N. Ayache et al. (Eds.): MICCAI 2012, Part II, LNCS 7511, pp. 395–403, 2012.

active contour [7] has been utilized for liver segmentation by R. S. Alomari *et al.* in [8] and by Chi *et al.* in [2]. The implicit deformable models, also called implicit active contours or level sets [9], have been utilized for liver segmentation as well. The statistical models have been received high interest from the investigators of liver segmentation approaches. They construct linear or non-linear models to represent the variation in liver shape and appearance like the approaches presented in [10,11,12]. In addition to statistical shape models, probabilistic atlases have been integrated into different liver segmentation approaches [13].

Despite this prosperous literature, we can conclude that the intensity- and deformable-based approaches were highly affected by the liver abnormalities. The statistical model- and probabilistic atlas-based approaches could enhance the results; however, they added a burden of model construction and matching. In this paper therefore, we present a knowledge-based liver segmentation approach. In this approach, we benefit from the high correlation between consequent slices of the same patient to define the shape constrains, and to estimate the statistical parameters of the liver and non-liver tissues. For initialization, the user segment one slice in the volume to define these constrains, and consequently they automatically updated from the nearby slices. A graph cuts algorithm based on the defined constrains is applied in a slice-by-slice manner to automatically segment the whole volume. Additionally, to reduce the computational time, we build the graph in a narrow band area defined from the adjacent slice. This proposed approach share the concept of constrains propagation with the method of *Lee et al.* [14]. However, the segmentation is performed from large to small liver cross sections which increases the ability of capturing separated and damaged liver parts. Moreover, shape and intensity constrains are integrated directly into the graph cuts segmentation algorithm and they are updated based on the segmentation results of the slices that have been processed so far.

The rest of this paper is organized as follows: in Sect. 2, the proposed approach is described. The evaluation results of the proposed approach are presented and discussed in Sect. 3. Finally, the paper is concluded in Sect. 4.

2 Proposed Segmentation Approach

The proposed segmentation approach mimics the human methodology in determining the boundary of liver. In this methodology, the correspondence between adjacent slices in CT image helps in alleviating the ambiguity of the liver boundary and in detecting the liver abnormalities. The whole procedure of the proposed approach is as follows:

Step-1: Performing image normalization in soft tissue window and then applying nonlinear diffusion filter to each slice.
Step-2: Selecting one slice containing nearly the largest liver cross section as the start slice and then define the liver object on it.
Step-3: Estimating initial shape, intensity, and graph cuts constrains from the start slice.

for all lower slices, starting from the start slice to the last one. **do**
Step-4: Define a narrow band around the liver object.
Step-5: Performing slice segmentation using shape-based graph cuts algorithm.
Step-6: Adding the segmentation results of this slice to the output volume.
Step-7: Updating shape, intensity, and graph cuts constrains according to the segmentation results of the current slice.
end for
for all upper slices, starting from the start slice to the first one. **do**
Repeat Step-4 and Step-5.
if the segmented object contains multiple parts **then**
Step-8: Selecting the left most one as the liver object.
end if
Repeat Step-6 and Step-7.
end for
Step-9: Applying the postprocessing procedure to the output volume.

2.1 Preprocessing

The first aim of this process is to map the raw CT data encoded in either twelve or sixteen bits to gray scale data encoded in eight bits. The mapping or normalization is performed in a soft tissue window determined by selecting the lower (Lo) and upper (Hi) bounds of the right distribution in the histogram of the raw CT data. This mapping is performed according to (1).

$$I_g(x,y) = \begin{cases} 0 & \text{if} \quad I_o(x,y) \leq Lo \\ \frac{255(I_o(x,y)-Lo)}{Hi-Lo} & \text{if } Lo \leq I_o(x,y) \leq Hi, \\ 255 & \text{if} \quad I_o(x,y) \geq Hi \end{cases} \tag{1}$$

where, I_o is the raw CT image, I_g is the produced gray level image.

After mapping the whole CT volume to a gray scale volume, a nonlinear diffusion filter [15] is applied to each 2D slice in the volume to reduce the noise and increase the liver homogeneity.

2.2 Estimation of the Shape and Intensity Constrains

The shape constrains are applied as a prior probability of the liver location, and the intensity constrains are defined as the probability of the liver intensity model at each pixel. These constrains are automatically determined for each slice according to the segmented liver in the previous slice. The estimation process is performed according to the following procedure.

1. Define; the binary image of liver segmentation in the start slice as $Temp_{str}$, the binary liver object in this slice as $objectinTemp_{str}$, the binary image of liver segmentation in the previous slice as $Temp_{prv}$, the binary liver object in this slice as $objectinTemp_{prv}$, the pixels belonging to the liver in the previous

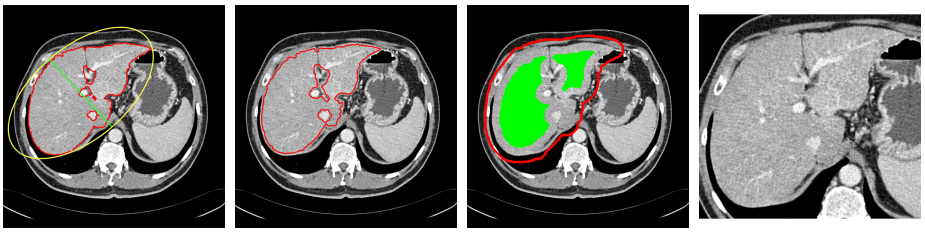

(a) (b) (c) (d)

Fig. 1. Constrains estimation, (a) sample previous slice (liver contour in red and the minor axis in green), (b) the contour of the estimated shape template shown on the current slice, (c) the estimated constrains for graph cut (object in green and background in red), and (d) the slice after applying the narrow band constrain

slice as $Liver_{prv}$, and the pixels not belonging to the liver in the pervious slice as $non - Liver_{prv}$.

2. Determine the minor axis of the ellipse that fit the object in $Temp_{prv}$ and denote it as m_{ax} (Fig. 1a).
3. Erode the $Temp_{prv}$ with a disk structuring element of radius round$(0.02 \times m_{ax})$ and considering the result as the shape template of the current slice (Fig. 1b). This erosion value has been decided after studying the average change of the minor liver axes in different cases.
4. If Area$(objectinTemp_{prv}) \geq 0.1 \times$ Area$(objectinTemp_{str})$,calculate the histogram of $Liver_{prv}$ and $non - Liver_{prv}$ as the intensity model; else, use the previously used intensity model.
5. Erode $Temp_{prv}$ with a disk structuring element of radius round$(0.1 \times m_{ax})$ and the result is considered as the object hard constrains in the graph cuts algorithm (Fig. 1c).
6. Dilate the $Temp_{prv}$ with a disk structuring element of radius $max(2,$ round$(0.1 \times m_{ax}))$. Then, the edge of the resulting binary template is determined and dilated with a disk structuring element of radius 1. The result of this step is considered as the background hard constrains in the graph cuts algorithm (Fig. 1c).
7. Define a narrow band window surrounding the liver object as the smallest rectangle fitting the dilated object calculated in Step 5 (Fig. 1d).

2.3 Segmentation Using Graph Cuts

The aim of this process is to find a labeling $A = \{A_1, A_2, , A_p, , A_{|P|}\}$ which minimize the the total energy function considering the estimated constrains as in (2).

$$E_T(A) = (1 - \lambda)R_D(A) + \lambda R_s(A) + \mu B(A), \tag{2}$$

where, μ determines the relative importance of the boundary term ,$B(A)$, versus the regional term and λ determines the relative importance of the data penalty, $R_D(A)$, versus the shape penalty ,$R_s(A)$. The data penalty reflects on how the

intensity of a pixel fits into the intensity model of the object (liver) and background (non liver tissues). The shape penalty is encoded as the prior probability of a pixel to be inside or outside the liver object. The data, shape, and boundary penalties are calculated as in (3), (4), and (5), respectively.

$$R_D\left(A_p\right) = \begin{cases} \frac{\log\left(pr\left(I_p \in \text{"}obj\text{"}\right)\right)}{\log\left(pr\left(I_p \in \text{"}obj\text{"}\right)\right)+\log\left(pr\left(I_p \in \text{"}bkg\text{"}\right)\right)} \text{ if } A_p = 1 \\ \\ \frac{\log\left(pr\left(I_p \in \text{"}bkg\text{"}\right)\right)}{\log\left(pr\left(I_p \in \text{"}obj\text{"}\right)\right)+\log\left(pr\left(I_p \in \text{"}bkg\text{"}\right)\right)} \text{ if } A_p = 0 \end{cases} \tag{3}$$

$$R_s\left(A_p\right) = \begin{cases} 1 - shape_{temp} \text{ if } A_p = 1 \\ shape_{temp} \quad \text{if } A_p = 0 \end{cases} \tag{4}$$

$$B_{pq} = e^{-\frac{\left|I_p - I_q\right|^2}{2\sigma^2}} \times \frac{1}{d(p,q)}, \tag{5}$$

where, $shape_{temp}$ is the estimated shape template of the objected (liver) in the current slice, I_p is the intensity value of a pixel p, $pr\left(I_p \in \text{“}obj\text{”}(\text{“}bkg\text{”})\right)$ is the probability of p to be an object("obj") or background ("bkg") pixel, and $d(p,q)$ is the Euclidian distance between pixels p and q.

This total energy function can be minimized efficiently using the graph cuts algorithm [16]. To achieve this goal, a graph with cut cost equaling the value of $E_T(A)$ is constructed using the edge weights defined in (6), (7), and (8). Furthermore, the hard constrains defined in Sect. 2.2 are implemented via infinity cost edges.

$$w_{sp} = \begin{cases} \infty & \text{if } p \in \text{"}obj\text{"} \\ 0 & \text{if } p \in \text{"}bkg\text{"} \\ (1-\lambda)R_D\left(A_p = 0\right) + \lambda R_s\left(A_p = 0\right) & otherwise \end{cases} \tag{6}$$

$$w_{pt} = \begin{cases} 0 & \text{if } p \in \text{"}obj\text{"} \\ \infty & \text{if } p \in \text{"}bkg\text{"} \\ (1-\lambda)R_D\left(A_p = 1\right) + \lambda R_s\left(A_p = 1\right) & otherwise \end{cases} \tag{7}$$

$$w_{pq} = B_{pq}(p,q), \tag{8}$$

w_{sp}, w_{pt} are the weight of the links to terminal nods, and w_{pq} is the weight of the link between two adjacent pixels.

2.4 Postprocessing

In this process, any tissue surrounded by the segmented liver tissue is added to the final segmentation which smoothed using a 3D filter. To achieve this goal the following procedure has been applied.

1. Perform hole filling to each 2D slice.
2. Perform binary image closing to the whole 3D volume using a ball structuring element of radius 3.
3. Perform hole filling to each 2D slice again.
4. Smooth the final volume by applying a binary median filter of $3 \times 3 \times 3$ size..

3 Results and Discussion

Data Sets: The data set used for evaluation is the MICCAI2007 grand challenge test set [17]. This test set contains 10 CT images acquired using variety of CT scanners. In some cases, the entire anatomy is rotated around the z-axes. Most images in this data set have liver abnormalities, including tumors, metastasis, and cysts of different sizes.

Parameter Setting: All parameters have been adjusted using 5 CT images having different characteristics; 3 from MICCAI2007 training data set and 2 from a local data set. Graph cuts parameter μ was set to 2. The parameter λ was set to 0.2. The parameter σ in the boundary term was dynamically selected from each slice as the average absolute intensity difference between the neighboring pixels ($\sigma = \frac{1}{|P|} \sum_{p \in P, q \in N_p} |I_p - I_q|$).

Evaluation Metrics: The proposed approach has been evaluated using the scoring system of MICCAI-2007 Grand Challenge workshop [2] which includes five metrics; Volumetric Overlap Error (VOE), Relative Volume Difference (RVD), Average Symmetric Surface Distance (ASD), Root Mean Square Symmetric Surface Distance (RMD), Root Mean Square Symmetric Surface Distance (RMD), and Maximum Symmetric Surface Distance (MSD). Moreover, the final precision score has been calculated according to the method presented by Heimann et. al. [2].

3.1 Experiments on Clinical Data

The segmentation approach has been implemented using Matlab environment on Windows-based personal computer with a Corei7(2.8GHz) processor and 6GB of memory. The evaluation results of the segmentation approach which calculated by the committee of the "3D Segmentation in the Clinic: A Grand Challenge" workshop of MICCAI2007 are shown in Table 1.

Comparative results of the proposed approach, the best automatic method (*Kainmüller et al.*) and all interactive methods reported by T. Heimann et. al. in [2] are shown in Table 2. As in [2], All approaches has been classified according to the time required for interaction. Less than 1 min was regarded as low interaction, less than 5 min as medium interaction, and more than 5 min as high interaction. Referring Table 2, the proposed approach share the best position with Beichel *et. al.* MBR. Additionally by referring the recent results on sliver07.org database [17], the proposed approach is in the third place of all methods. However, the proposed approach is significantly faster, requires less amount of interaction, and does not require extensive manual refinement. The automatic method of Kainmüller *et. al.* achieved this results by using an extensive training set of 112 liver shapes to build a statistical shape model (SSM) consists of around 7.000 landmarks. The total score of the same method was 73 when the number of training shapes used to build the SSM was 43 [10].

Since the shape and intensity constrains are estimated in a case-specific manner, the proposed approach is robust for liver shape variations and existence of liver abnormalities. Fig. 2 show that, the proposed approach can efficiently

Table 1. Evaluation results of the proposed approach

Case	VOE		RVD		ASD		RMD		MSD		Total Score	Time (sec.)	
	[%]	Score	[%]	Score	[mm]	Score	[mm]	Score	[mm]	Score		Initial	Total
#1	5.2	80	2.4	87	0.7	82	1.4	81	14.7	81	82	35	221
#2	5.9	77	5.0	74	0.8	80	1.7	76	19.4	74	76	40	223
#3	3.9	85	2.2	88	0.7	83	1.1	84	14.0	82	84	37	218
#4	5.0	80	2.5	86	0.7	81	1.4	80	10.4	86	83	36	122
#5	6.1	76	1.2	94	1.0	76	1.9	74	21.5	72	78	36	118
#6	5.8	78	0.7	96	0.8	79	1.8	74	20.1	74	80	37	204
#7	3.8	85	1.5	92	0.5	87	1.2	84	16.0	79	85	38	170
#8	6.2	76	1.1	94	1.0	75	2.3	68	22.2	71	77	35	113
#9	4.2	84	1.2	94	0.5	87	1.2	83	16.0	79	85	37	284
#10	4.5	82	0.5	98	0.6	86	1.2	84	11.5	85	87	36	108
Average	5	80	1.8	90	0.7	82	1.5	79	16.6	78	81.7	36.7	178.1
Std. Dev.	0.9	3.6	1.3	7.0	0.18	4.3	0.4	5.5	4.1	5.3	3.8	1.5	60.8

Table 2. Comparative results of the proposed segmentation approach

Method	VOE		RVD		ASD		RMD		MSD		Final	Runtime
	[%]	Score	[%]	Score	[mm]	Score	[mm]	Score	[mm]	Score	Score	[min]
Beichel *et. al.* MBR(high)	5.2	80	1.0	91	0.8	80	1.4	80	15.7	79	82	36
Proposed approach(low)	**5**	**80**	**1.8**	**90**	**0.7**	**82**	**1.5**	**79**	**16.6**	**78**	**82**	**3**
Kainmüller *et. al.*(Automatic)	6.1	76	−2.9	85	0.9	76	1.9	74	18.7	75	77	15
Beck and Aurich(high)	6.6	74	1.8	88	1.0	74	1.9	73	18.5	76	77	7
Dawant *et. al.*(med)	7.2	72	2.5	86	1.1	73	1.9	74	17.1	77	76	20
Second rater	6.4	75	4.7	75	1.0	75	1.8	75	19.3	75	75	
Lee *et. al.*(low)	6.9	73	1.3	88	1.1	73	2.1	71	21.3	72	75	7
Beichel *et. al.* CBR(med)	6.5	74	1.1	90	1.1	72	2.5	66	23.4	69	74	31
Wimmer *et. al.*(med)	8.1	68	6.1	68	1.3	67	2.2	69	18.7	75	69	4 − 7
Slagmolen *et. al.*(med)	10.4	59	3.7	70	2.0	50	5.0	34	40.5	47	52	60
Beichel *et. al.*(low)	14.3	48	3.1	62	3.6	34	7.9	24	49.2	38	41	30

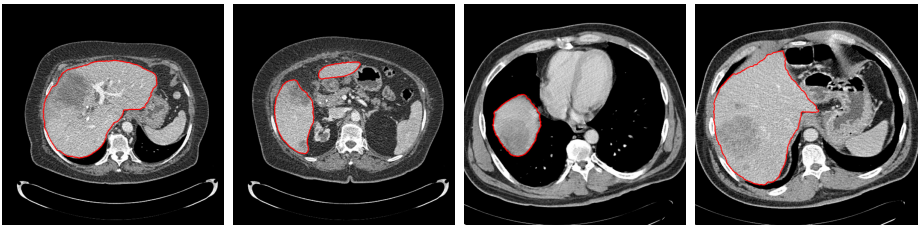

(a) (b) (c) (d)

Fig. 2. Segmentation results of cases containing large and dense liver tumors

extract the liver in different cases containing large and dense tumors. Referring Table 1, the average performance of the proposed approach (81.7) cab be regarded as closer to the reference manual segmentation than the human performance (75) [2]. Small deviation of these scores shows the ability of the proposed approach to deal with extreme cases as well as easy and moderate cases. The processing time required to segment a CT volume ranges from $2-5$ minutes and it is significantly less than the manual or other conventional segmentation methods. In general, the proposed approach can efficiently utilize the anatomical knowledge of the liver to achieve accurate segmentation results.

4 Conclusion

In this work, we proposed a novel shape-based approach for liver segmentation in portal-venous CT images using a case-specific knowledge. In which, the relation between consequent slices of the same image is exploited to estimate the shape and intensity information of the liver. Then, this information is integrated into the graph cuts algorithm to segment the whole CT image. Unlike the other shape-based segmentation approaches which use training data to build a statistical model, the proposed technique does not require prior model construction. Accordingly, it is not restricted to the trained model, and it can be applied when there is no training data available. The evaluation results demonstrated the high precision of the proposed approach. It efficiently estimates the liver boundary even with the existence of large and dense liver abnormalities. The utilization of a case-specific knowledge increases the ability of the proposed approach to deal with difficult and atypical liver shapes. Additionally, it removes the burden of model construction and matching. A low processing time required by the proposed approach makes it suitable for clinical application.

References

1. Campadelli, P., Casiraghi, E., Esposito, A.: Liver segmentation from computed tomography scans: A survey and a new algorithm. Artificial Intelligence in Medicine 45, 185–196 (2009)
2. Heimann, T., Ginneken, B.V., Styner, M.A., Arzhaeva, Y., Aurich, V., Bauer, C., Beck, A., Becker, C., Beichel, R., Bekes, G., Bello, F., Binnig, G., Bischof, H., Bornik, A., Cashman, P.M.M., Chi, Y., Córdova, A., Dawant, B.M., Fidrich, M., Furst, J.D., Furukawa, D., Grenacher, L., Hornegger, J., Kainmüller, D., Kitney, R.I., Kobatake, H., Lamecker, H., Lange, T., Lee, J., Lennon, B., Li, R., Li, S., Meinzer, H.P., Németh, G., Raicu, D.S., Rau, A.M., van Rikxoort, E.M., Rousson, M., Ruskó, L., Saddi, K.A., Schmidt, G., Seghers, D., Shimizu, A., Slagmolen, P., Sorantin, E., Soza, G., Susomboon, R., Waite, J.M., Wimmer, A., Wolf, I.: Comparison and Evaluation of Methods for Liver Segmentation From CT Datasets. IEEE Trans. Med. Imag. 28(8), 1251–1265 (2009)
3. Rusko, L., Bekes, G., Fidrich, M.: Automatic segmentation of the liver from multi- and single-phase contrast-enhanced CT images. Medical Image Analysis 13, 871–882 (2009)
4. Foruzana, A.H., Zoroofia, R.A., Horib, M., Satoc, Y.: Liver segmentation by intensity analysis and anatomical information in multi-slice CT images. International Journal of CARS 4(3), 287–297 (2009)
5. Tibamoso, G., Rueda, A.: Semi-automatic Liver Segmentation From Computed Tomography (CT) Scans based on Deformable Surfaces. SLIVER07 Results (October 2009), `http://sliver07.isi.uu.nl/results/20091022201318/description.pdf`
6. Gao, J., Kosaka, A., Kak, A.: A Deformable Model for Automatic CT Liver Extraction. Academic Radiology 12(9), 1178–1189 (2005)
7. Xu, C., Prince, J.: Snakes, shapes, and gradient vector flow. IEEE Trans. Image Process. 7(3), 359–369 (1998)

8. Alomari, R.S., Kompalli, S., Chaudhary, V.: Segmentation of the Liver from Abdominal CT Using Markov Random Field model and GVF Snakes. In: Proc. International Conference on Complex, Intelligent and Software Intensive Systems, pp. 293–298 (2008)
9. Sethian, J.A.: Level Set Methods and Fast Marching Methods, 2nd edn., pp. 1–74. Cambridge University Press (1996)
10. Kainmuller, D., Lange, T., Lamecker, H.: Shape Constrained Automatic Segmentation of the Liver based on a Heuristic Intensity Model. In: Proc. MICCAI Workshop on 3-D Segmentation in Clinic: A grand Challenge, pp. 109–116 (2007)
11. Afifi, A., Nakaguchi, T., Tsumura, N., Miyake, Y.: A Model Optimization Approach to the Automatic Segmentation of Medical Images. IEICE Trans. on Information and Systems E93-D(4), 882–889 (2010)
12. Linguraru, M.G., Pura, J.A., Chowdhury, A.S., Summers, R.M.: Multi-organ Segmentation from Multi-phase Abdominal CT via 4D Graphs Using Enhancement, Shape and Location Optimization. In: Jiang, T., Navab, N., Pluim, J.P.W., Viergever, M.A. (eds.) MICCAI 2010, Part III. LNCS, vol. 6363, pp. 89–96. Springer, Heidelberg (2010)
13. Okada, T., Shimada, R., Hori, M., Nakamoto, M., Chen, Y.W., Nakamura, H., Sato, Y.: Automated Segmentation of the Liver from 3D CT Images Using Probabilistic Atlas and Multilevel Statistical Shape Model. Academic Radiology 15(11), 1390–1399 (2008)
14. Lee, J., Kim, N., Lee, H., Seo, J.B., Won, H.J., Shin, Y.M., Shin, Y.G., Kim, S.-H.: Efficient liver segmentation using a level-set method with optimal detection of the initial liver boundary from level-set speed images. Computer Methods and Programs in Biomedicine 88, 26–38 (2007)
15. Weickert, J., Romeny, B.M., Viergever, M.A.: Efficient and Reliable Schemes for Nonlinear Diffusion Filtering. IEEE Trans. Image Process. 7(3), 398–410 (1998)
16. Boykov, Y., Veksler, O., Zabih, R.: Fast approximate energy minimization via graph cuts. IEEE Trans. on Pattern Anal. Mach. Intell. 23(11), 1222–1239 (2001)
17. Heimann, T., Ginneken, B.V., Styner, M.A.: Segmentation of the Liver 2007 (SLIVER07), `http://sliver07.isi.uu.nl/` (last visted: June 10, 2012)